Coupling light to periodic nanostructures

Driessen, E.F.C.

Chapter 6

Waveguide modes in solid-state index-matched metal hole arrays

We investigate the surface-plasmon modes of a metal hole array covered with a thin layer of glass. The glass layer diminishes the asymmetry of the structure, which leads to degenerate surface plasmon modes propagating on both sides of the metal hole array, when the glass layer is sufficiently thick. Besides the plasmon resonances, we observe a number of sharp dips in the transmission spectra, that are caused by waveguide modes in the glass layer on top of the metal hole array. Calculations of the dispersion of these guided modes show perfect agreement with the measurements.

This chapter is based on M. J. A. de Dood, E. F. C. Driessen, D. Stolwijk, M. P. van Exter, M. A. Verschuuren, and G. W. 't Hooft, *Index matching of surface plasmons*, Proc. SPIE **6987**, 698713 (2008).

6.1 Introduction

For sensing applications, it may be interesting to design structures in which the plasmons on different sides are index matched. In this chapter, we attempt to achieve index matching of the surface plasmon resonances on both sides of the metal hole array that was investigated in Ch. 5. For this purpose, it was covered with a thin (~ 400 nm) layer of sol-gel glass. This layer serves as an index matching layer and should make the surface plasmons that propagate on different sides of the metal film indistinguishable. The thin layer of glass however acts as a waveguide. The modes of this waveguide cause extra sharp resonances to occur in the transmission spectra. In section 6.2 we investigate these waveguide modes. In section 6.3 we discuss the effect of the finite thickness of the glass layers on the effective index of the surface plasmon modes, and show that it is possible to fabricate a structure where the surface-plasmon modes on both sides of the gold layer are degenerate.

6.2 Waveguide modes

In Fig. 6.1, we compare the transmission spectra for the metal hole array with (top) and without (bottom) the dielectric layer deposited on top of the structure. A number of changes is observed. Most notably, the increase of intensity of the peak that is associated with the (1,0) surface plasmon resonance on the glass side of the structure. The resonances belonging to the air side of the structure are shifted in wavelength, and a number of new features are observed in the spectra.

Figure 6.2 shows the measured transmission as function of the angle of incidence. Several strong, relatively broad, minima (black lines in Fig. 6.2) are clearly visible. These minima in transmission are associated with the Fano-type line shape caused by the coupling to a surface-plasmon mode. Two such modes can be observed, which correspond to a surface plasmon mode propagating on the substrate side and a surface plasmon mode propagating on the side covered with the dielectric layer. These modes can still be distinguished because the AF45 substrate has a higher refractive index ($n \approx 1.52$) than the sol-gel material ($n \approx 1.40$), making the structure slightly asymmetric.

In addition to the surface plasmon modes that are clearly visible, the new features that are observed in Fig. 6.1 also clearly show angular dispersion. For instance, at normal incidence a resonance appears at a wavelength of 700 nm, which cannot be explained by a surface plasmon mode. The extra resonances are characterized by a sharp symmetric dip instead of the asymmetric line

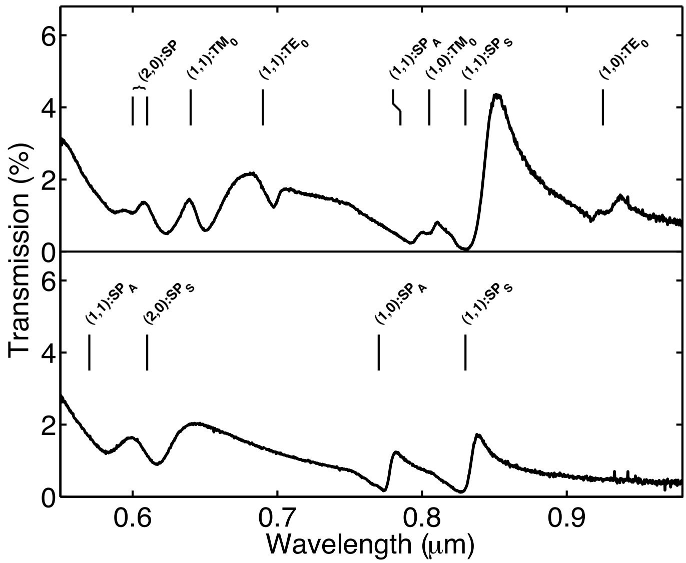

Figure 6.1. Measured transmission of the metal hole array of Ch. 5. The bottom curve shows the transmission spectrum for the structure without a glass layer on top, the top curve shows the transmission spectrum when a $\sim$ 400 nm thick layer of glass is deposited on top of the structure. The positions of the different resonances are indicated with lines, as well as the character of the resonances.

shape of the surface plasmon modes, and are caused by coupling to a waveguide mode supported by the dielectric superstrate [62]. Similar to the case of surface plasmons, the resonance condition to excite a mode is given by

$$\vec{k}_{\parallel} = \vec{\beta}_m + \vec{G}, \tag{6.1}$$

where $\vec{\beta}_m$ is the propagation constant of the mode, and $\vec{k}_{\parallel}$ and $\vec{G}$ are defined as in Ch. 5. For this layered structure, $\vec{\beta}_m$ has to be found numerically. The modes can be classified as either transverse electric (TE) or transverse magnetic (TM) depending on whether the E-field or the H-field vector is perpendicular to the surface normal of the structure. Following the notation of Ref. [63], we define the x-direction as perpendicular to the interface and the z-direction as the propagation direction of the guided mode. The dielectric constant $\epsilon(x)$ of our structure is stepwise continuous and equal to ϵ_1 for $0 \leq x$, ϵ_2 for $-d \leq x \leq 0$ and equal to 1 for $x \leq -d$. Here, d is the thickness of the dielectric layer, and ϵ_1, ϵ_2 and ϵ_3 are the dielectric constants of the metal, the dielectric layer and the dielectric above the structure, respectively. The metal-to-dielectric

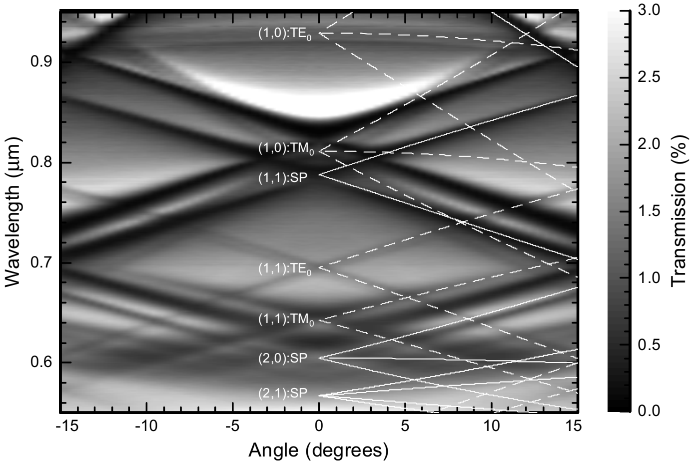

Figure 6.2. Grayscale plot of the measured transmission of a metal hole array covered with a dielectric layer as function of angle of incidence. The lines in the figure correspond to the calculated position of the different resonances. Each of the resonances corresponds to a specific reciprocal lattice vector and has an additional label to indicate the nature of the mode; i.e. surface plasmon (SP), fundamental TE waveguide mode (TE_0) or fundamental TM waveguide mode (TM_0).

interface is positioned at $x = 0$. The H-field of the m-th order TM mode that propagates in the positive z-direction can be written as

$$\vec{H}_m(\vec{r}, t) = \vec{H}_m(x)\, \mathrm{e}^{i(\omega t - \beta_m z)}, \tag{6.2}$$

where β_m is a propagation constant, that can be interpreted as the component of the wavevector parallel to the interface. For modes that are guided, the H field is confined either to the metal-to-dielectric interface (surface plasmon) or to the dielectric layer. Outside the region of the dielectric layer, the field $\vec{H}_m(x)$ decays exponentially. The H-field points in the y-direction (i.e., parallel to the interface), and it is given by

$$H_m(x) = \begin{cases} \frac{\epsilon_1 S_2}{\epsilon_2 S_1} \exp(-S_1 x) & 0 \leq \ x \\ \frac{\epsilon_1 S_2}{\epsilon_2 S_1} \cosh(S_2 x) - \sinh(S_2 x) & -d \leq \ x \ \leq 0 \\ \left[\frac{\epsilon_1 S_2}{\epsilon_2 S_1} \cosh(S_2 d) + \sinh(S_2 d)\right] \times & \\ \qquad \exp[S_3(x+d)] & \quad x \ \leq -d \end{cases} \tag{6.3}$$

where the transverse momentum in the layer with dielectric constant ϵ_i is given by $S_i = \sqrt{\beta_m^2 - (\omega^2/c^2)\epsilon_i}$. A mode of this form can only exist when the boundary conditions from Maxwell's equations are fulfilled at $x = 0$ and $x = d$, leading to the condition

$$\tanh(S_2 d) = -\frac{S_2}{\epsilon_2}\left(\frac{S_1}{\epsilon_1} + \frac{S_3}{\epsilon_3}\right) \Bigg/ \left(\left(\frac{S_2}{\epsilon_2}\right)^2 + \frac{S_1}{\epsilon_1}\frac{S_3}{\epsilon_3}\right). \tag{6.4}$$

This last equation can be used to numerically find the propagation constant β_m as function of frequency for all TM modes, including the surface plasmon mode. A similar approach can be applied to find all TE waveguide modes.

The curves in Fig. 6.2 are the numerically calculated resonance conditions for the surface plasmon on the sol-gel side (solid curves) and the waveguide modes in the structure (dashed curves). The calculated resonances due the surface plasmon on the substrate side are slightly red shifted and have been omitted from the figure for reasons of clarity. Each of the calculated resonances in the figure is labeled by a combination of reciprocal lattice vector and an identifier to indicate the nature of the mode. The modes are classified as a surface plasmon (SP), a fundamental TE waveguide mode (TE_0) or a fundamental TM waveguide mode (TM_0). In our calculation, we adjusted the thickness d of the sol-gel layer to get good agreement with the measured data and find a value of 480$\pm$10 nm. For this layer thickness, the cut-off frequencies of the higher order TE and TM waveguide modes are beyond the frequency range probed in the experiment.

6.3 Effects of layer thickness

The formalism discussed in the previous section can be used to design structures where the surface-plasmon resonances on both sides of the structures are index matched, by using a dielectric layer. A numerical algorithm is used to find the propagation constant β of the surface plasmon at a given wavelength as function the layer thickness d of the dielectric layer. This calculation is done for the surface plasmon modes on the "air" ($n = 1.0$) side of the structure as well as on the substrate ($n = 1.52$) side of the structure. In both cases, the dielectric layer has a refractive index of 1.4. This calculation allows to find the minimum required thickness of the dielectric layer, on each side, that is needed to create a structure in which the surface plasmon modes on the two interfaces are indistinguishable.

Figure 6.3 shows the real part of the calculated effective index, defined as $n_{\text{eff}} = \beta_m(\omega)c/\omega$, for gold covered with a dielectric film, as a function of the layer thickness d, for a wavelength of 800 nm (solid curve). The dotted curves show similar calculations for slightly different wavelengths of 700 nm and 900 nm. We have included results for both sides of the metal film, with insets next to the curves to show the configuration that corresponds to the curves. For a thin dielectric layer inserted between the metal and air, the surface plasmon propagates mostly in the air and the effective index is close to that of a surface plasmon propagating on a bare air-to-gold interface. When the layer thickness is increased, the effective index approaches that of a surface plasmon on a single dielectric-to-metal interface. From the figure it is clear that this situation is reached for a layer thickness ~ 500 nm. As expected, the required thickness becomes smaller for shorter wavelengths.

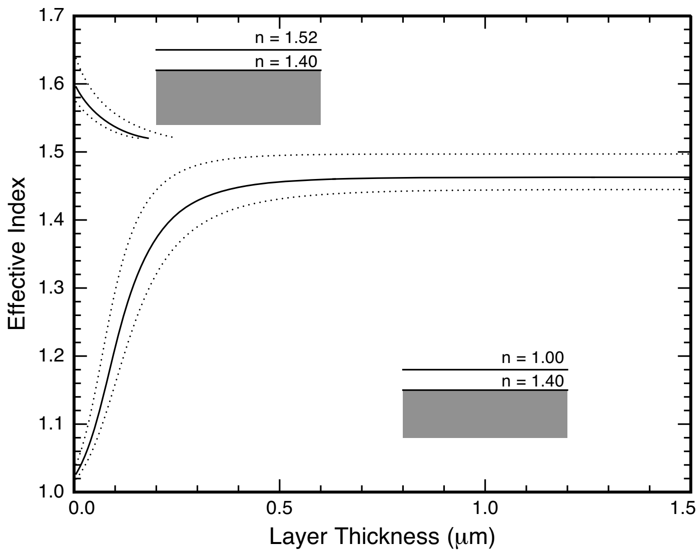

Figure 6.3. Effective index for a gold interface covered with a dielectric film, as a function of the thickness of the dielectric layer. The dielectric layer has a refractive index $n = 1.40$. Results are shown for an ambient with a lower refractive index ($n = 1.00$), and with a higher refractive index ($n = 1.52$). The solid curves are calculated for a wavelength of 800 nm. The dotted curves indicate the change when the wavelength is 700 nm and 900 nm.

The effective index for the configuration that corresponds to the substrate side of the metal film behaves differently. As shown in the figure, the curves start at an effective index of a surface plasmon on a glass-to-gold interface. As long as a very thin layer of dielectric is used, the effective index of the surface plasmon is always larger than that of the dielectric with the highest ϵ, for frequencies below the plasmon frequency [64]. If the layer thickness is increased this is no longer the case and bound modes cease to exist for thicknesses larger than 200 nm. At this point, the effective index of the surface plasmon mode becomes equal to the refractive index of the substrate and the surface mode transforms into a leaky mode. However, for a sufficiently thick dielectric layer, the coupling to radiation modes will be weak and the mode resembles the plasmon mode of a single glass-to-gold interface with $n = 1.4$. Based on the calculation of the surface plasmon mode on the air side, we estimate that the typical thickness required for this regime is also around 500 nm for a wavelength of 800 nm.

In Fig. 6.4, we show a grayscale plot of the transmission of such a symmetric structure. This structure was fabricated on a sol-gel glass layer of thickness 1000 nm, and after the deposition of the gold layer, another thick sol-gel glass layer was deposited on top of the structure. Again, the waveguide modes that are supported by the thick glass layer on top are clearly visible. From a fit of the waveguide mode dispersion, discussed before, we determined the thickness of the top layer to be $\sim$ 2100 nm. Besides the waveguide modes, the surface plasmon resonances are also clearly visible, as the dark diagonal bands. The surface plasmon modes on either side of the hole array have become indistinguishable.

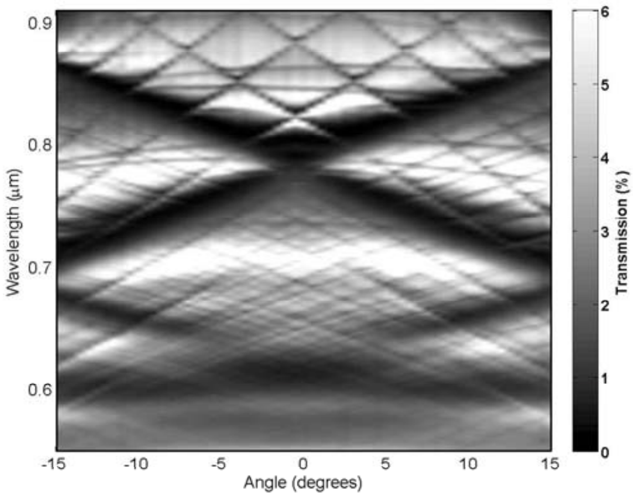

Figure 6.4. Gray scale plot of the measured transmission of a metal hole array covered with a $\sim$ 2100 nm thick dielectric layer, as a function of angle of incidence and wavelength. The surface-plasmon modes on either side of the hole array (broad dark bands) have become indistinguishable. The waveguide modes that are supported by the dielectric layer are clearly visible as sharp black lines.

6.4 Conclusion

In this chapter, we have shown that it is possible to make the resonances that correspond to surface plasmons that propagate on either side of a metal hole array indistinguishable. To achieve this, a sufficiently thick layer of glass needs to be deposited on top of the hole array. If the glass layer is too thin, the exponential tail of the surface plasmon will extend beyond the layer, which lowers the propagation constant of the surface plasmon. The transmission spectra of the metal hole arrays with a glass layer on top show a number of extra resonances, that are caused by resonant coupling to the waveguide modes that are sustained by this glass layer. Calculation of the dispersion of these modes gives perfect agreement with the measurements, and allowed us to determine the thickness of the glass layer. The surface-plasmon resonances in the (close to) index-matched structures change intensity and width. This change is further investigated in the next chapter.